

COMPUTER SIMULATIONS OF ACCELERATED PARTICLES IN THE RIKEN SSC

A. Goto, N. Nakanishi and Y. Yano
 The Institute of Physical and Chemical Research
 Wako shi, Saitama 351, Japan

Summary

Results of computer simulations for the following problems are presented: 1) effects of an rf magnetic field on a beam; 2) possibility of single turn extraction by off centered injection; 3) a method to measure a two dimensional motion of an orbit center using three radial differential probes.

1. Introduction

We have made various computer simulations of accelerated particles for the RIKEN SSC using the field data which were measured for the sector magnet in 1982.¹

One of these simulations was to study numerically the mechanism of phase compression and expansion due to an rf magnetic field. In this work, it was found that the rf magnetic field affects the behaviors not only of longitudinal emittance but also of radial one. Matching condition at injection in the longitudinal phase space was also studied.

For single turn extraction, in some cases it is available to use an off centered acceleration instead of using a first harmonic field in the extraction region. We have studied its possibility.

It is one of the most important diagnoses in the actual operation to measure the precise position of the orbit center. We have found the means with which the position of an orbit center in two dimensional directions is determined using three radial differential probes.

In this paper, we will discuss the effects of the rf magnetic field on a beam and the off-centered acceleration for single turn extraction. The algorithm to determine the position of an orbit center will also be described.

2. Effect of an rf magnetic field

The rf electric field that has a nonuniform radial distribution along the dee gap is accompanied by an rf magnetic field. In an isochronous cyclotron, when a beam is accelerated by such an electric field, its phase width is varied by the effect of this rf magnetic field.^{2,3}

The rf resonator of the RIKEN SSC is designed to produce an acceleration voltage with a radially increasing distribution. In our case, therefore, it is important to take into account the rf magnetic field in the computer simulations. In the following subsections, the effect of the rf magnetic field on the beam behavior and its related problems will be presented.

2.1 Energy resolution

Taking into account the change of the phase width due to the nonuniform radial distribution of acceleration voltage V/R , the final energy deviation (ΔE_f) of

a particle with an initial energy deviation (ΔE_i) and phase (φ_i) is given by⁴

$$\Delta E_f = a \cdot \Delta E_i + b \cdot \varphi_i^2, \quad (1)$$

where a is the ratio of the final to the initial voltage (V_f/V_i) and b is proportional to the radial integration of $R/V(R)^3$. This relation was verified by the computer simulation. The final energy resolution strongly depends on the shape of the radial distribution of the rf voltage. A radially increasing distribution is desirable for a good energy resolution.

As mentioned elsewhere^{5,6} in this conference, we have modified the design of the resonator, which was reported in the preceding conference. The rf voltage distribution of the old design has a dip in intermediate radii at higher frequencies (30-45 MHz). Because of this dip the energy resolution is not much higher than that in the case of a uniform distribution in spite of the ratio $V_f/V_i \sim 2$. In the new design, this dip can be eliminated and the distribution will be monotonously increasing. It is expected that the distribution will be uniform at 20 MHz and almost linearly increasing with $V_f/V_i \sim 2$ at 45 MHz. Consequently, at 45 MHz, the value of b in the new design becomes smaller by a factor of about 2 than that in the old one. The energy resolution will get better or phase acceptance will get wider.

2-2. φ - δ matching

It is important to find the optimal relation for φ_i and δ_i (δ_i is the initial momentum resolution) in order to get a beam with high energy resolution. If the emittance in (φ, δ) phase space at the injection point of the SSC is supposed to be an ellipse, the best final energy resolution can be obtained under such a condition that the initial ellipse is erect and the final energies of both the particles with $(0, -\delta_i)$ and with $(\pm \varphi_i, 0)$ are equal to each other. The above relation is different according to the shape of the radial distribution of rf voltage. From eq.(1) it is given by $\delta_i = 4 \varphi_i^2$ for a uniform radial distribution, while it is given by $\delta_i = 1.12 \varphi_i^2$ for a linearly increasing distribution with the ratio V_f/V_i of 2. (The ratio R_f/R_i is 4 in our case.)

In the case that the (φ, δ) phase-ellipse from the injector linac (RILAC)⁷ is given by $\varphi_L = \pm 6^\circ$ and $\delta_L = \pm 0.075\%$ (estimated values), $\varphi_i = \pm 2.4^\circ$ and $\delta_i = \pm 0.19\%$ from the above relation for the rf voltage distribution with $V_f/V_i = 2$ and the conservation law of emittance ($\delta_i = 1.12 \varphi_i^2$ and $\varphi_i \delta_i = \varphi_L \delta_L$). Fig. 1 a) shows the transformation of phase ellipse when a beam is injected under the above matching condition. In Fig. 1 b) is shown the transformation in the mismatching case that $\varphi_i = \pm 4.7^\circ$ and $\delta_i = \pm 0.096\%$. These figures indicate the importance of the matching in (φ, δ) phase space to get a higher energy resolution beam. The design of a beam bunching system in the injection line should be made by taking into account the above matching condition.

Fig. 1. Transformation of longitudinal phase ellipse when a beam is injected a) with and b) without the matching condition.

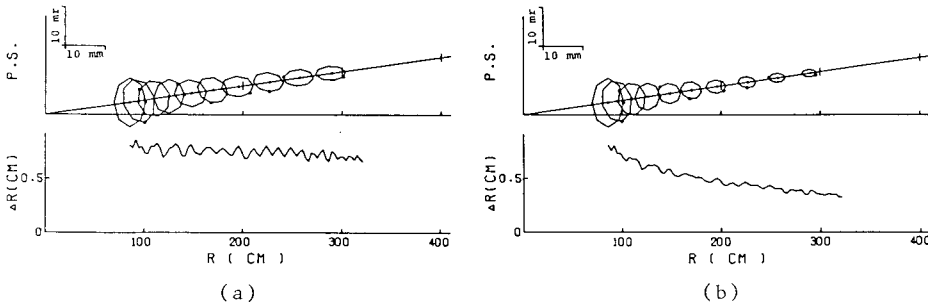
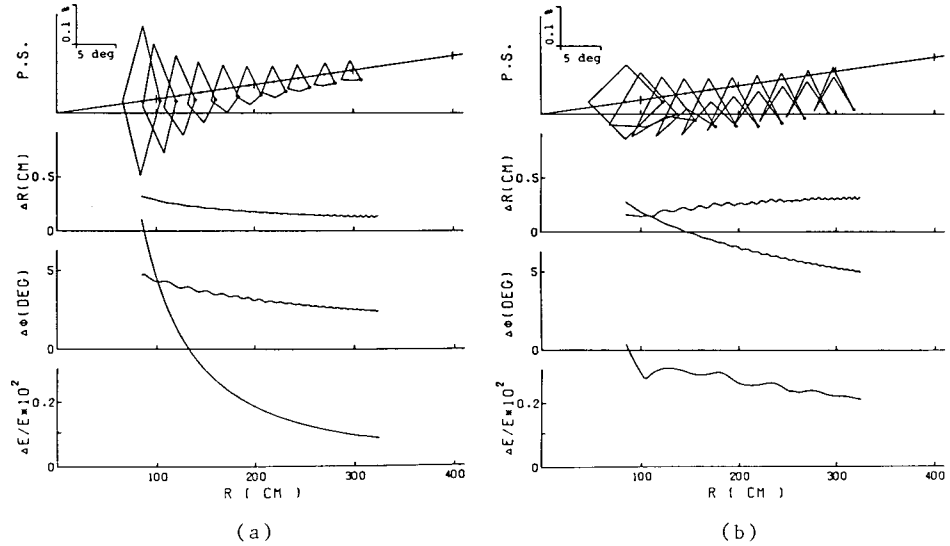


Fig. 2. Transformation of radial phase ellipse a) in the case of incorporating the rf magnetic field and b) in the case of deliberately omitting it.

2-3. (r, r') phase ellipse

The rf magnetic field plays an important role in predicting the emittance in (r, r') phase space as well. To investigate this role, computer simulations were made in two cases: with and without the effect of the rf magnetic field. Fig. 2 shows simulations of the transformation of the radial phase ellipse and the beam width. In Fig. 2 a) is presented the result in the case of incorporating the rf magnetic field and in Fig. 2 b) the result in the case of deliberately omitting it. The rf voltage was assumed to be a linearly increasing distribution with $V_f/V_i = 4$. The striking point is that in the case of b) the reduction rate of the emittance is larger than in the case of a) by a factor of about 4. The implication of these results is that the rf magnetic field is indispensable in the computer simulations to describe the behavior of a beam not only in longitudinal phase space but also in radial one.

3. Acceleration of off-centered beam

For a beam which does not have enough turn spacing in the extraction region, we have some ways to achieve single turn extraction. As one of them, acceleration of an off-centered beam has been examined. The turn separation of the off centered beam shows an oscillatory pattern because of rotation of the orbit center around the machine center. The radial position of an off-centered particle is given by ⁸

$$R = R_c(n, \phi_{cp}) + A \cdot \cos[\psi_0 + 2\pi \int_0^n (\nu_r(R) - 1) dn], \quad (2)$$

where R_c is the radial position at turn number n of a centered particle with a central position phase ϕ_{cp} , and A the oscillation amplitude. ψ_0 is the oscillation

phase at injection and ν_r the radial focusing frequency.

In eq. (2), the amplitude A and initial phase ψ_0 are functions of the radial displacement and the angle of the off-centered orbit with respect to the well-centered orbit at injection. The integral term depends on the acceleration voltage. Firstly, the values of the radial displacement and the angle were searched to give as large oscillation amplitude as possible under the restriction that the off centered beam clears all the injection elements. Secondly, the acceleration voltage was adjusted so that the maximum turn separation can be obtained at the extractor.

Calculation was done for a proton beam of an injection emittance of 20 mm·mrad. Initial energy spread and central position phase were set to be zero. The rf magnetic field was also taken into account. Behavior of four parameters in the radial and longitudinal phase spaces is shown in Fig. 3 for the off-centered 9 MeV proton beam. The difference between well- and off-centered beams was found to be very small except that energy resolution degrades slightly in off-centered case. In Fig.4 are shown radial phase ellipses in the last few turns at several azimuthal positions near the extractor.

The 10 MeV proton beam encounters a resonance of radial focusing frequency $\nu_r = 4/3$ at the energy of 188 MeV. It is known that this is a quadratic, nonlinear, intrinsic resonance. We confirmed that its influence is negligibly small for the well centered beam. As seen in Fig. 5, on the other hand, it is not so small for the off-centered beam. This is due to the effective extension of a radial beam size. Therefore this method is not always suitable for the 10 MeV proton beam.

There are many parameter sets to make extraction of the off-centered beam possible. We have to employ the parameter set which does not make beam quality worse.

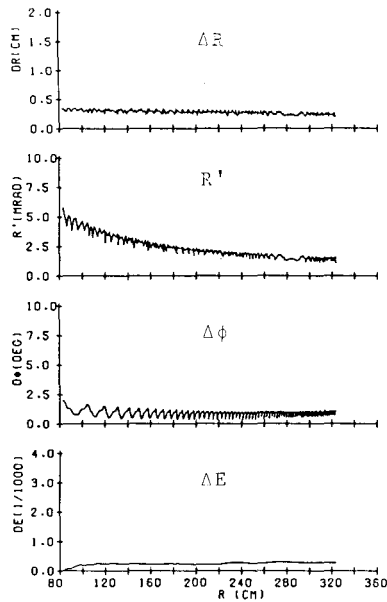


Fig. 3. Variation of beam property in radial and longitudinal phase spaces for a 9 MeV off-centered proton beam.

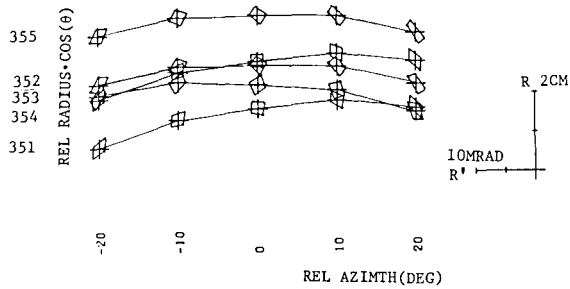


Fig. 4. Radial phase ellipses in the last five turns. Abscissa is a relative azimuth. The 0 deg. corresponds to a valley center. Ordinate is the product of radius and cosine of a relative azimuth. Numerals at the left show turn numbers.

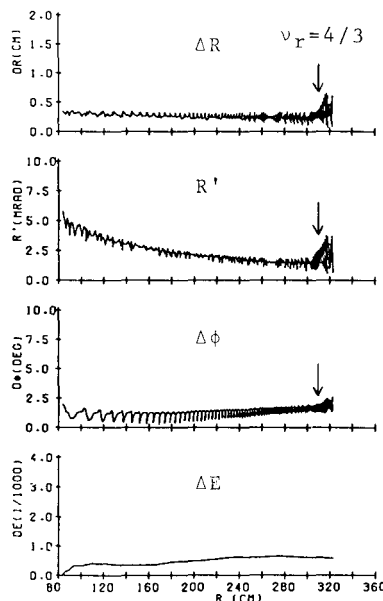


Fig. 5. Variation of beam property in radial and longitudinal phase spaces for a 10 MeV off-centered proton beam. The effect induced by a resonance $\nu_r = 4/3$ is observed.

4. A method to measure two-dimensional motion of orbit center with three radial differential probes

It quite facilitates the tuning of acceleration orbit, e.g. centering and off centering of the beam, to measure the positions of orbit center in both x and y directions. Such measurement necessitates, in principle, at least three radial differential probes. As shown in Fig. 1 of Ref. 5, in our SSC the radial differential probes are arranged at three azimuthal positions of sector edge lines. We describe below the method of measurement of the position of orbit center with these probes, which is the extension of the VICKSI's method⁸.

We define the valley mid line and the dee mid line as x and y- axes, respectively. In the preceding paper⁹ we presented the condition for the acceleration equilibrium orbit (AEO). This orbit is depicted in Fig. 6. The radial gain Δr is the difference in radii

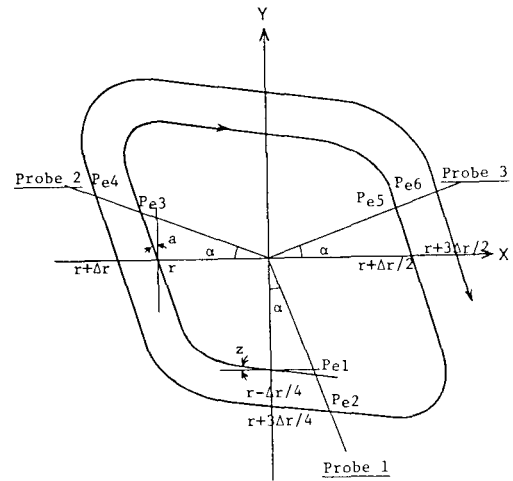


Fig. 6. Acceleration equilibrium orbit (AEO) and configuration of three radial differential probes. In case of our SSC, $\alpha = 20^\circ$.

between the successive AEO's in one turn. The angles, α and z , come from the above condition. These are given by

$$\alpha = \frac{\Delta r}{4 \sin(\pi \nu_r / 2)} \left(\frac{r r'_0}{r_0} \right), \quad (3)$$

$$z = \alpha \cdot \cos\left(\frac{\pi}{2} \nu_r\right), \quad (4)$$

where r_0 (radial displacement) and r'_0 (angle) represent the principal axes of the eigen-ellipse at the radius of r on the x-axis, and ν_r the corresponding radial focusing frequency. From Fig. 6 the radii of the AEO at each azimuth of probe, $Pe_1 - Pe_6$, are given by

$$Pe_1 = \frac{1}{C} (1+z) \left(r - \frac{1}{4} \Delta r \right) = \frac{1}{C} \left(r - \frac{1}{4} \Delta r \right), \quad (5)$$

$$Pe_2 = \frac{1}{C} (1+z) \left(r + \frac{3}{4} \Delta r \right) = \frac{1}{C} \left(r + \frac{3}{4} \Delta r \right), \quad (6)$$

$$Pe_3 = \frac{1}{C} (1+at) r = \frac{1}{C} \left(r - \frac{1}{4} t f \Delta r \right), \quad (7)$$

$$Pe_4 = \frac{1}{C} (1+at) (r + \Delta r) = \frac{1}{C} \left\{ r + \left(1 + \frac{1}{4} t f \right) \Delta r \right\}, \quad (8)$$

$$Pe_5 = \frac{1}{C} (1-at) \left(r + \frac{1}{2} \Delta r \right) = \frac{1}{C} \left\{ r + \left(\frac{1}{2} - \frac{1}{4} t f \right) \Delta r \right\}, \quad (9)$$

$$Pe_6 = \frac{1}{C} (1-at) \left(r + \frac{3}{2} \Delta r \right) = \frac{1}{C} \left\{ r + \left(\frac{3}{2} - \frac{1}{4} t f \right) \Delta r \right\}, \quad (10)$$

where $c = \cos\alpha$, $t = \tan\alpha$ and

$$f = \frac{1}{\sin(\pi\nu_r/2)} \left(\frac{rr_0}{r_0} \right), \quad (11)$$

Because the value of z is negligible, it is taken to be null in eqs. (5) and (6). We also neglect the term, $(\Delta r)^2$, in eqs. (7)-(10).

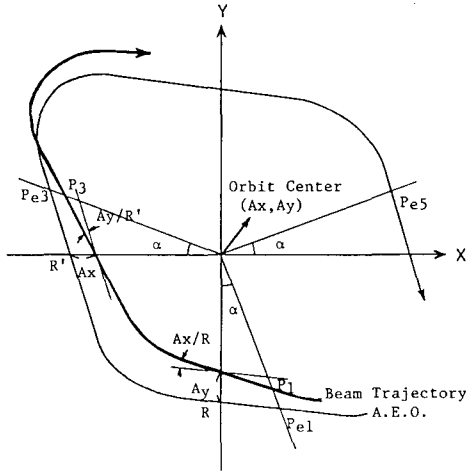


Fig. 7. Beam trajectory with respect to the AEO, the orbit center at the radius of R on the x-axis being given by (A_x, A_y) .

Fig. 7 shows the beam trajectory with respect to the AEO; the orbit center existing at the coordinate of (A_x, A_y) . We neglect the rotation of the orbit center during about $1\frac{1}{2}$ turns. From Fig. 7 the radius (P_1) of the position where the probe 1 catches the beam is given by

$$P_1 = P_{e1} + \frac{1}{C} (tA_x - A_y). \quad (12)$$

In the same way,

$$P_2 = P_{e2} + \frac{1}{C} (tA_x - A_y). \quad (13)$$

$$P_3 = P_{e3} - \frac{1}{C} (A_x - tA_y). \quad (14)$$

$$P_4 = P_{e4} - \frac{1}{C} (A_x - tA_y). \quad (15)$$

$$P_5 = P_{e5} + \frac{1}{C} (A_x + tA_y). \quad (16)$$

$$P_6 = P_{e6} + \frac{1}{C} (A_x + tA_y). \quad (17)$$

From eqs. (5)-(17) the following relations are obtained.

$$A_x = \frac{1}{8} \cos\alpha (P_6 + 3P_5 - 3P_4 - P_3) + \frac{1}{8} \sin\alpha (P_6 - P_5 + P_4 - P_3), \quad (18)$$

$$A_y = \frac{1}{2} \cdot \frac{1}{1 + \tan\alpha} \{ 2A_x \tan\alpha - \cos\alpha (P_1 + P_2 - P_3 - P_5) \}. \quad (19)$$

In order to verify the reliability of these formulae, we simulated this three-probe measurement of the orbit center as well as the four-probe measurement; the four probes being arranged on the x- and y-axes. The calculation was made for $^{12}\text{C}^{6+}$ with injection energy of 50.8 MeV. The first harmonic field of 15 G was applied. The value of f changes from 1.31 to 1.7 with the radius. In the calculation it was fixed to be 1.5. Fig. 8 shows the results a) in the first fifteen

turns and b) in the last seven turns obtained by the three (solid line) and four (dashed line) probe measurements.

It was found that the three probe measurement mentioned here is quite reliable in tracing the two dimensional motion of the orbit center.

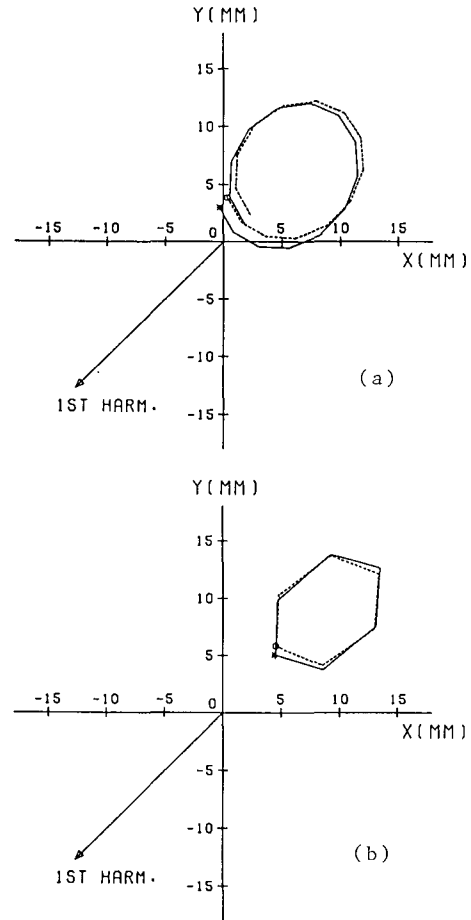


Fig. 8. Comparison of the three (solid line) and four (dashed line) probe measurements. a) in the first fifteen turns (injection region). b) in the last seven turns (extraction region).

References

1. S.Motonaga et al., Proc. of Int. Conf. on Magnet Technology, Grenoble, 1983, to be published.
2. R.W.Müller and R.Mahrt, Nucl. Instr. and Meth., 86 (1970) 241.
3. W.Joho, Particle Accelerators, 6 (1974) 41.
4. G.Hinderer, Proc. of the 9th Int. Conf. on Cyclotrons and their Applications, Caen, (1983) 327.
5. H.Kamitsubo, 'The RIKEN Linear Accelerator - Cyclotron System', this conference.
6. T.Fujisawa et al., 'Design of the RF System of RIKEN SSC', this conference.
7. M.Kase et al., 'Variable Frequency Linac, RILAC, as an injector of Separated Sector Cyclotron', this conference.
8. W.M.Schulte, The Theory of Accelerated Particles in AVF Cyclotrons, thesis, Eindhoven University of Technology (1978).
9. A.Goto et al., Proc. of the 9th Int. Conf. on Cyclotrons and their Applications, Caen, (1983) 439.